Int. J. Heat Mass Transfer. Vol. 26, No. 4, pp. 567–582, 1983
Printed in Great Britain

0017–9310/83/040567–16 $03.00/0

TRANSIENT HEAT CONDUCTION UNDER PLASMA CONDITIONS

E. BOURDIN and P. FAUCHAIS
Laboratoire de thermodynamique, UER Sciences, Université de Limoges, France

and

MAHER BOULOS
Département de génie chimique, Université de Sherbrooke, Québec, Canada

(*Received* 3 *November* 1981 *and in revised form* 30 *July* 1982)

Abstract—A theoretical analysis was made of the different phenomena encountered and the assumptions involved in the calculation of the heat transfer rate to a single sphere under plasma conditions. In the presence of steep temperature gradients it is shown that if the integral mean thermal conductivity of the plasma is used in the evaluation of the heat transfer coefficient, the Nusselt number for the conduction heat transfer between the plasma and the particle is equal to 2.0. The results also show that the relaxation time of the thermal boundary layer around the particle is negligible compared to its transient heating-up time. Computations were carried for particles of different diameters (20–100 μm) and materials (Al_2O_3, W, Si, Cu . . .) immersed in plasmas of argon, nitrogen and hydrogen over the temperature range 4000–10 000 K. These show that for Biot numbers greater than 0.02, temperature differences as high as 1000 K can develop between the surface and the center of the particle even for a particle as small as 20 μm in diameter. In a few cases where the heat flux is particularly high (hydrogen plasma at 10 000 K) the surface temperature of a 100 μm alumina particle can reach the boiling point of alumina (4000 K) while its center is still in the solid state. The results of a relatively simple analysis show that, except for a particle with a surface temperature above 2000 K immersed in an argon or a nitrogen plasma below 4000 K, radiation heat losses from the particle to the surroundings are negligible compared to the conductive heat flux from the plasma to the particle.

NOMENCLATURE

a, b, constants;
Bi, Biot number, k/k_s;
C_1, constant, equation (2);
C_p, specific heat at constant pressure [J kg^{-1} K^{-1}];
C_l, C_s, specific heat of the particle in the liquid and solid phase, respectively [J kg^{-1} K^{-1}];
d_0, particle diameter [m];
h, heat transfer coefficient [W m^{-2} K^{-1}];
k, thermal conductivity [W m^{-1} K^{-1}];
$\bar{k}$, integrated mean thermal conductivity of the plasma gas [W m^{-1} K^{-1}];
k_l, k_s, thermal conductivity of the particle in liquid and solid phase, respectively [W m^{-1} K^{-1}];
Nu, Nusselt number, $hd_0/\bar{k}$;
q, heat flux to the surface of the particle [W m^{-2}];
q_{rad}, radiative heat losses from the particle [W m^{-2}];
r, distance in the radial direction [m];
r_e, radius of the particle under vaporization conditions [m];
r_m, radius of the melting front [m];
r_∞, radius at which the gas temperature reaches the free stream plasma temperature [m];
R_0, particle radius [m];
Re, Reynolds number, $\rho u d_0/\mu$;
t, time [s];
T, temperature [K];
T_s, particle surface temperature [K];
T_∞, free stream plasma temperature [K].

Greek symbols

α_l, α_s, thermal diffusivity of the liquid and of the solid particle, respectively [m^2 s^{-1}];
Δt_f, time necessary for the particle to melt [s];
ΔT_s, temperature difference between the surface and the center of the particle [K];
λ_l, λ_s, latent heat of the particle respectively for vaporization and for fusion [MJ kg^{-1}];
ρ, ρ_l, ρ_s, density of the plasma, of the liquid, and of the solid particle, respectively [J kg^{-1} K^{-1}];
δ, boundary layer thickness [mm];
ε, emissivity of the particle;
σ, Stephan–Boltzman constant.

1. INTRODUCTION

THE THERMAL treatment of powders under plasma conditions represents one of the important applications of plasma technology which lead to a number of successful industrial developments. Plasma spray coating [1–3] and powder spheroidization [4] are typical examples.

In the plasma spraying operation, the coating material is introduced in the form of a fine powder in a DC plasma jet as shown in Fig. 1. As the particles are entrained by the plasma gas they are heated, molten and accelerated to a velocity of the order of a few

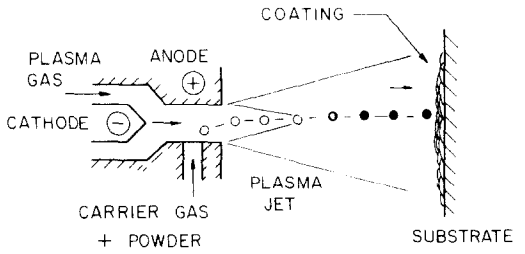

FIG. 1. Powder injection in a DC plasma jet as commonly used in plasma spray coating.

hundred meters per second. Upon impaction of the liquid droplets on the substrate, they flatten and form a lamella structured thin film of the coating material. The quality of the deposit obtained depends to a large extent on the particle temperature and velocity at the moment of impaction. A particle which reaches the substrate while still in the solid state would not flatten and thus increase the brittleness and the porosity of the coating.

A considerable effort has been devoted to the optimization of the powder injection conditions to insure the complete melting of the particles in the plasma jet. A number of fundamental studies have been made of the plasma–particle heat transfer [5–8] and of the modelling of the trajectories and temperature histories of the particles as they are injected in the plasma jet [9–17]. These, however, have not always been consistent in the assumptions made and the relative importance attributed to the different heat transfer mechanisms involved. For example, only a few investigations dealt with the problem of internal heat propagation in the particles [12, 13, 15, 16] while the others assumed the particles to be at a uniform temperature with negligible internal temperature gradients. The presence of steep temperature gradients across the boundary layer around the particle and its effect on the transfer properties of the gas has often been dealt with in a rather empirical fashion. Without exception, all investigations have used steady-state correlations for the calculation of the conductive and convection heat transfer coefficients between the plasma and the particles under transient conditions.

While a number of these assumptions could well be justified under certain conditions, there remains considerable ambiguity about the limits of their validity and the role of the different heat transfer mechanisms in the overall transfer process.

In an attempt to clarify this situation, the present investigation has set as its objective an answer to the following specific questions:

(1) To what extent does the method used account for the variations of the transfer properties of the plasma across the boundary layer and can it influence the estimated heat transfer rates?

(2) How long is the relaxation time of the thermal boundary layer around the particle compared to its transient residence time in the plasma?

(3) Under which conditions can internal heat conduction have an important influence on the overall heat transfer rate to the particle?

(4) What are the possible temperature differences that can develop between the surface and the center of the particle under different conditions?

The approach used is theoretical. It is based on the solution of the corresponding transfer equations for a single spherical particle under different conditions. In order to maintain its relevance to the original plasma spray coating problem, the computations were carried out for the particle sizes, materials, and plasma conditions typically used in plasma spray coating operations. A summary of the materials studied and their corresponding physical and thermodynamic properties are given in Table 1. The study was carried out at atmospheric pressure with argon, nitrogen and hydrogen as the plasma gases at temperatures in the range from 4000 to 10000 K. Since under typical operating conditions the particle Reynolds number is rather small ($Re_p < 100$), the plasma–particle heat transfer analysis was limited to conduction heat transfer.

An extension of the results to include convective heat transfer can be made relatively simply. The contribution of radiative heat transfer to the overall energy balance around the particles was also neglected since, as shown later, it represented only a small percentage of the overall heat transfer rate to, or from, the particle.

2. PLASMA–PARTICLE CONDUCTIVE HEAT TRANSFER

2.1. *Effect of steep temperature gradients*

During the transient heating of a particle under plasma conditions, the surface temperature of the particle can be about 1000–2000 K while the ambient plasma temperature is 10000 K. The presence of such a

Table 1. Materials studied and their corresponding physical and thermodynamic properties

Material	Density ($kg\ m^{-3}$)	Molecular Weight	Melting point (K)	Boiling point (K)	Specific heat ($J\ kg^{-1}\ K^{-1}$)	Latent heat of fusion ($MJ\ kg^{-1}$)	Thermal conductivity ($W\ m^{-1}\ K^{-1}$)
Si	2330	28	1685	2628	905	1.80	108.0
SiO_2	2320	60	2000		1157	0.14	1.5
Al_2O_3	4000	102.0	2326	4000	1242	1.00	6.3
Cu	8930	63.5	1356	2840	425	0.20	398.0
Ni	8900	58.7	1727	3005	541	0.30	73.3
W	19350	183.8	3680	6200	170	0.19	110.0

steep temperature gradient across the boundary layer can have an important effect on the heat transfer rates. The question dealt with in this section is simply: at which temperature should the fluid property values be evaluated?

To answer this question, consider the steady-state conductive heat transfer between the plasma and an isolated spherical particle. The governing equation can be written in spherical coordinates as follows:

$$\frac{1}{r^2}\frac{\mathrm{d}}{\mathrm{d}r}\left(r^2 k\frac{\mathrm{d}T}{\mathrm{d}r}\right) = 0. \tag{1}$$

Integrating equation (1) between the surface of the particles ($r = R_0$ and $T = T_s$) and any other point r, we obtain

$$r^2 k\frac{\mathrm{d}T}{\mathrm{d}r} = C_1 \tag{2}$$

and

$$\int_{T_s}^{T(r)} k(T)\,\mathrm{d}T = C_1\left(\frac{1}{R_0} - \frac{1}{r}\right) \tag{3}$$

where C_1 is a constant.

Equations (2) and (3) can be used to calculate the heat flux to the surface of the particle

$$q = k\frac{\mathrm{d}T}{\mathrm{d}r}\bigg|_{r=R_0} \tag{4}$$

or

$$q = \frac{C_1}{R_0^2} = \frac{1}{R_0^2}\int_{T_s}^{T(r)} k(T)\,\mathrm{d}T \Big/ \left(\frac{1}{R_0} - \frac{1}{r}\right) \tag{5}$$

for $r = r_\infty$, the radius at which the gas temperature reaches the free stream plasma temperature T_∞, we obtain

$$q = \frac{1}{R_0^2}\int_{T_s}^{T_\infty} k(T)\,\mathrm{d}T \Big/ \left(\frac{1}{R_0} - \frac{1}{r_\infty}\right) \tag{6}$$

for $r_\infty \gg R_0$ the above equation simplifies to

$$q = \frac{1}{R_0}\int_{T_s}^{T_\infty} k(T)\,\mathrm{d}T. \tag{7}$$

The heat flux can be expressed in terms of a heat transfer coefficient, h, as follows:

$$q = h(T_\infty - T_s). \tag{8}$$

From equations (7) and (8) we obtain

$$h = \frac{1}{R_0(T_\infty - T_s)}\int_{T_s}^{T_\infty} k(T)\,\mathrm{d}T. \tag{9}$$

The above equation can be rewritten in terms of the Nusselt number, $Nu = hd_0/\bar{k}$, we obtain,

$$Nu = \frac{2}{\bar{k}(T_\infty - T_s)}\int_{T_s}^{T_\infty} k(T)\,\mathrm{d}T \tag{10}$$

which reduces to the well-known expression $Nu = 2.0$, commonly used at moderate and low temperature conditions, if we use the thermal conductivity of the gas, $\bar{k}$, as its integral mean value across the boundary layer defined as follows;

$$\bar{k} = \frac{1}{(T_\infty - T_s)}\int_{T_s}^{T_\infty} k(T)\,\mathrm{d}T. \tag{11}$$

Equation (11) was used earlier by Bonnet [8] and other workers for the calculation of the average thermal conductivity of the gas in the thermal boundary layer under plasma conditions.

It is interesting to note that if $k(T)$ is a linear function of temperature $k(T) = aT + b$ the above equation can be integrated to give

$$\bar{k} = \frac{1}{(T_\infty - T_s)}\left[\frac{aT^2}{2} + bT\right]_{T_s}^{T_\infty} \tag{12}$$

which simply reduces to the commonly used practice to evaluate the property values at the arithmetic mean temperature of the surface and the free-stream temperatures, i.e.

$$\bar{k} = k(\bar{T}),$$

with

$$\bar{T} = \frac{T_\infty + T_s}{2} \tag{13}$$

The application of equation (11) can be considerably simplified by splitting the integral with respect to some reference temperature $T_0 = 300$ K, as follows:

$$\bar{k} = \frac{1}{(T_\infty - T_s)}\left[\int_{300}^{T_\infty} k(T)\,\mathrm{d}T - \int_{300}^{T_s} k(T)\,\mathrm{d}T\right] \tag{14}$$

or

$$\bar{k} = \frac{1}{(T_\infty - T_s)}[I(T_\infty) - I(T_s)] \tag{15}$$

where, $I(T)$, which is known as the 'heat conduction potential', is defined as

$$I(T) = \int_{300}^{T} k(T)\,\mathrm{d}T. \tag{16}$$

Based on the available literature data, the integrated thermal conductivity, $I(T)$, was calculated using equation (16) for different gases at atmospheric pressure and the results given in Fig. 2 together with the corresponding values of the thermal conductivity as function of temperature.

2.2. *Boundary layer relaxation time*

The question treated in this section is how long is the relaxation time of the thermal boundary layer around the particle, compared to its transient residence time in the plasma?

Let us consider a particle of radius R_0, and uniform temperature T_s, suddenly immersed in a plasma at a temperature T_∞. Following a similar development as that given in the previous section, it can be shown that equation (6) gives rise to the following relation for the

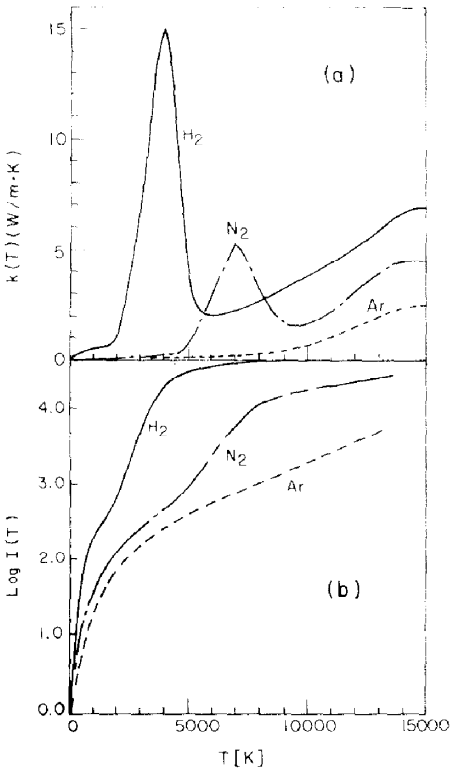

FIG. 2. Thermal conductivity (a) and the integrated thermal conductivity (b) for different gases at atmospheric pressure as function of temperature

$$\left[I(T) = \int_{300}^{T} k(T)\,\mathrm{d}T\right].$$

instantaneous Nusselt number:

$$Nu(t) = \frac{2r_\infty}{r_\infty - R_0} \tag{17}$$

where r_∞ is the limit of the thermal boundary layer around the particle. In other words, it is the radius at which the gas temperature is equal to 0.99 of the plasma temperature.

At time $t = 0 + \varepsilon$ where ε is a small increment of time, r_∞ will not be much larger than R_0 and the Nusselt number could be considerably greater than 2.0. As the particle receives heat from the plasma, the thickness of the boundary layer, $\delta = (r_\infty - R_0)$, will increase leading to the limiting case where for $r_\infty \gg R_0$, $Nu = 2.0$.

The heat transfer equation governing the transient development of the thermal boundary layer around the particle can be written as follows:

$$\rho C_p \frac{\partial T}{\partial t} = \frac{1}{r^2}\frac{\partial}{\partial r}\left(kr^2\frac{\partial T}{\partial r}\right) \tag{18}$$

where ρ, C_p and k are the plasma density, specific heat and thermal conductivity, respectively. Equation (18) could be solved using the following boundary conditions:

$$r = R_0, \quad t = 0, \quad T(t) = T_{s_0}, \quad t > 0,$$

$$T(t) = T_{s_0} + \frac{3}{\rho_s C_s R_0}\int_0^t k\left(\frac{\partial R}{\partial r}\right)\Big|_{r=R_0} \mathrm{d}t, \tag{19a}$$

$$r > R_0, \quad t = 0, \quad T(r,t) = T_\infty,$$

$$\delta(t) = 0,$$

$$t > 0, \quad T(\delta,t) = T_\infty,$$

$$\left(\frac{\partial T}{\partial r}\right)_{r=\delta} = 0. \tag{19b}$$

The results expressed in terms of the instantaneous Nusselt number as function of time, obtained for a particle with a diameter of 100 μm immersed in a nitrogen plasma at 10 000 K are given in Fig. 3. In this figure, two curves are given. One is for the case where the particle surface temperature was assumed to vary

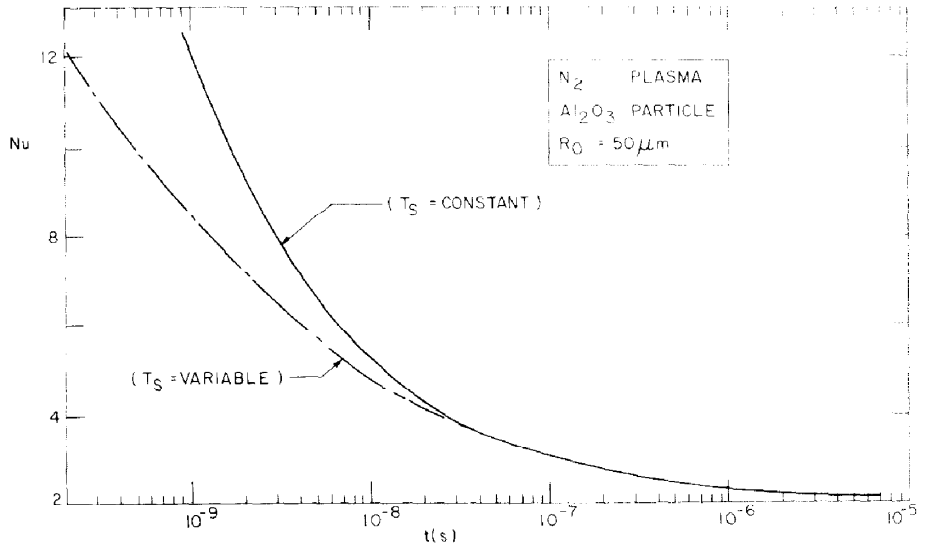

FIG. 3. Variation of the instantaneous Nusselt number as function of time for a 100 μm diameter particle in a nitrogen plasma at 10 000 K.

with time according to equation (19a), i.e. at $r = R_0$ and $t > 0$, $T(t) =$ variable. The second curve on Fig. 3 represents an approximate solution where the surface temperature of the particle was assumed to be constant, i.e. $r = R_0$ and $t > 0$ $T(t) = T_{s_0}$.

In either case, it is noticed that the instantaneous Nusselt number drops rapidly with time and attains its asymptotic value of 2.0 in about 1 μs from the time the particle has been immersed in the plasma. Since in most plasma spray coating applications, the residence time of the particles in the plasma jet is of the order of a few milliseconds, it appears that, as far as the boundary layer relaxation is concerned, the use of a Nusselt number of 2.0 for the calculation of the conductive heat transfer rate to the particle is quite adequate.

3. INTERNAL HEAT TRANSFER IN THE PARTICLES

As mentioned earlier, most of the studies of particle heating under plasma conditions have neglected the effects of internal heat conduction in the particle on the overall transfer process. This section will deal with the effects of internal conduction on the heating-up time of particles in the absence or presence of phase change. An attempt will be made to define an appropriate parameter that can be used to determine *a priori* when internal heat transfer in the particles can be neglected and when it must to be taken into account.

For comparison, computations will first be made for a particle with an infinite thermal conductivity, i.e. uniform particle temperature. This will be followed by calculations for particles with a finite thermal conductivity in the absence of phase change, and finally for particles with a finite thermal conductivity in the presence of phase change.

3.1. *Heat transfer to a particle with an infinite thermal conductivity*

The evolution of the temperature of a particle with an infinite thermal conductivity suddenly immersed in a plasma stream can simply be calculated by an energy balance on the particle. Assuming a Nusselt number of 2.0 and neglecting radiation losses from the particle it can be easily shown that

$$\frac{dT_s}{dt} = \frac{-12\bar{k}}{\rho_s C_s d_0^2}(T_s - T_\infty) \tag{20}$$

where k is the mean thermal conductivity of the gas, given by equation (11), ρ_s and C_s are the density and the specific heat of the particle, respectively. Since k and C_s are functions of temperature, equation (2) has to be solved using standard numerical techniques such as the Runge–Kutta–Merson method. As a first approximation, if $\bar{k}$ and C_s are assumed to be constant, it is possible to obtain the following exact solution:

$$\frac{T_s - T_\infty}{T_0 - T_\infty} = \exp\left(\frac{12\bar{k}t}{\rho_s C_s d_0^2}\right). \tag{21}$$

As expected, equation (21) shows that the particle temperature rises the faster the higher the thermal conductivity of the gas and the lower the specific heat and the diameter of the particle.

Computations were next carried out to solve equation (20) taking into account the variations of either $\bar{k}$, C_s or both with the temperature of the particle. Typical results obtained for a 100 μm diameter alumina particle immersed in a nitrogen plasma are given in Fig. 4. It is interesting to note that the results are essentially the same in either case and hardly differ from the exact solution given by equation (21). This is mainly due to the relatively small change in the temperature of the

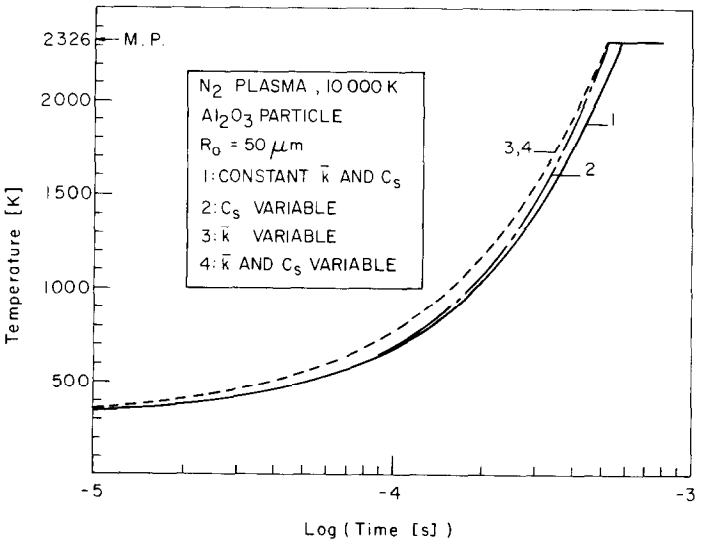

FIG. 4. Temperature history for a 100 μm diameter alumina particle immersed in a nitrogen plasma at 10 000 K (neglecting internal heat conduction).

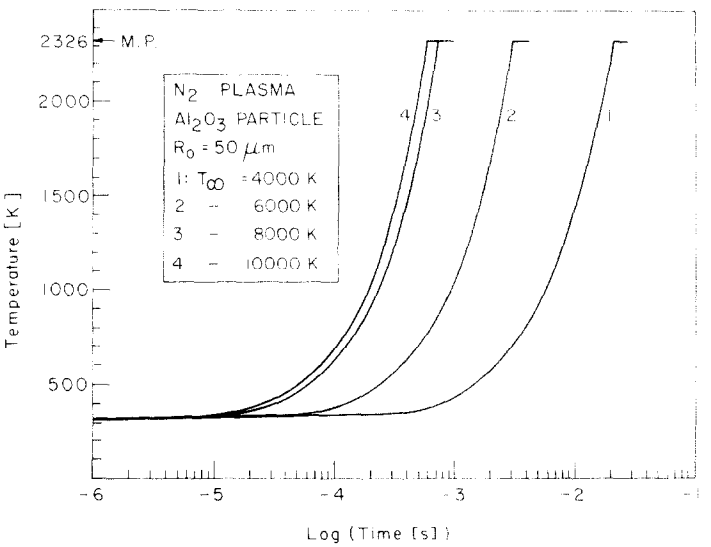

FIG. 5. Temperature histories for 100 μm diameter alumina particles immersed in a nitrogen plasma at different temperatures (neglecting internal heat conduction).

particle compared to the temperature difference between the plasma and the particle.

Calculations were also carried out using equation (21) to determine the effects of variations of the plasma temperature (4000–10 000 K), plasma gas (H_2, N_2, Ar), particle material (Ni, Si, Al_2O_3, W, SiO_2) and diameter (20, 60, 100, 200, 400 μm), on the temperature history of the particles as they are suddenly immersed in the plasma. The results are given in Figs. 5–8, respectively. It should be pointed out that while the computations were stopped as the particle reached its melting point, the constant temperature portion at the end of each of these curves represents the time that would be taken by the particle for complete fusion, calculated as follows:

$$(\Delta t)_{\text{fusion}} = \frac{\lambda_s \rho_s d_0^2}{12\bar{k}(T_\infty - T_s)} \tag{22}$$

where λ_s is the latent heat of fusion of the particle. It is noticed from Fig. 5 that there is a very substantial improvement in the heating efficiency of the particles with the increase of the temperature of the plasma from 4000 to 6000 K. The effect is far smaller between 8000 and 10 000 K. This supports the generally accepted rule that for diatomic gases there is relatively little to gain, from a particle heating point of view, by using a plasma at a temperature higher than the dissociation

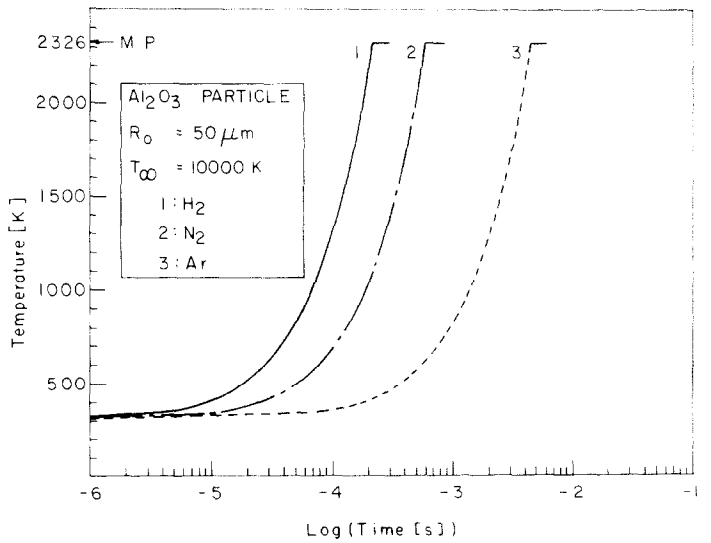

FIG. 6. Temperature histories for 100 μm diameter alumina particles immersed in different plasma gases at 10 000 K (neglecting internal heat conduction).

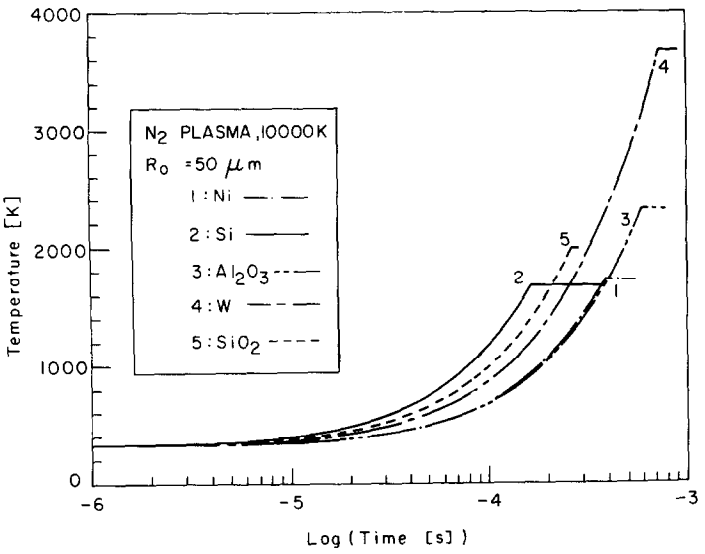

FIG. 7. Temperature histories for 100 μm diameter particles of different materials immersed in a nitrogen plasma at 10 000 K (neglecting internal heat conduction).

temperature of the gas (8000–10 000 K for N_2 and 5000–7000 K for H_2 at atmospheric pressure). This is due to the steep increase of $\bar{k}$ associated with the dissociation of the gas (Fig. 2). The results given in Fig. 6 show that by proper selection of the plasma gas considerable improvement in the heat transfer rate to the particles can be achieved, thus reducing the heating time. In fact the increase of the mean thermal conductivity of the plasma from 0.07 to 4.4 associated with the change from an argon to a hydrogen plasma results in a reduction of the time required to melt a 100 μm diameter alumina particle from 4×10^{-3} to about 2×10^{-4} s.

3.2. *Heat transfer to a particle with a finite thermal conductivity in the absence of phase change*

In this section we examine the effect of internal heat conduction in the particle on the temperature distribution and its overall heating rate. The calculations are based on the following assumptions:

(1) The particle is spherical with a finite but constant specific heat and thermal conductivity.

(2) The particle has a uniform initial temperature, T_0, before it is suddenly immersed in a plasma of a temperature T_∞.

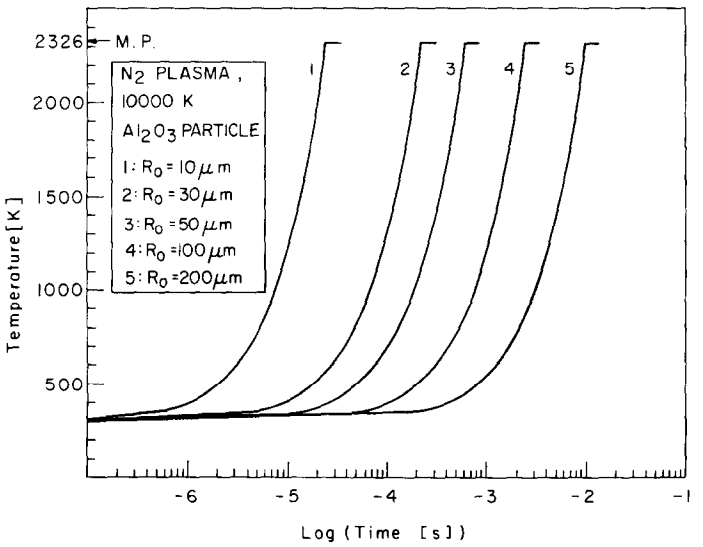

FIG. 8. Temperature histories for alumina particles of different diameters immersed in a nitrogen plasma at 10 000 K (neglecting internal heat conduction).

(3) Negligible radiation losses from the particle to the surroundings.

(4) The particle temperature is followed only to the point where its surface reaches the melting point of the material.

Based on the above assumptions, the equation governing the transient heat transfer in the particle can be written as follows:

$$\frac{1}{\alpha_s}\frac{\partial T}{\partial t} = \frac{1}{r^2}\frac{\partial}{\partial r}\left(r^2\frac{\partial T}{\partial r}\right) \tag{23}$$

where α_s is the thermal diffusivity of the particle material, $\alpha_s = [k_s/\rho_s C_s]$. Equation (23) can be solved with the following boundary conditions:

$$t = 0, \quad 0 < r < R_0, \quad T(r,t) = 300\ \text{K}, \tag{24a}$$

$$t > 0, \quad r = 0 \quad \left.\frac{\partial T}{\partial r}\right|_{r=0} = 0, \tag{24b}$$

$$r = R_0 \quad k_s \left.\frac{\partial T}{\partial r}\right|_{r=R_0} = q \tag{24c}$$

where q is the external heat flux to the surface of the particle given by equation (8) with a Nusselt number of 2.0.

$$q = \frac{2\bar{k}}{d_0}(T_\infty - T_s). \tag{25}$$

The system of partial differential equations was solved using an implicit finite-difference method. The results obtained for a 100 μm diameter alumina particle suddenly immersed in a nitrogen plasma at 10 000 K are given in Figs. 9(a) and (b) in terms of the temperature history of the particle and the internal transient temperature profiles, respectively.

It can be noted from Fig. 9(a) that the temperature difference between the surface of the particle and its center can be as much as 1250 K. It is also noted that the results of computations using the 'simple model', assuming an infinite thermal conductivity of the particle, i.e. uniform particle temperature, represents relatively well the mean temperature of the particle. This can be attributed to the fact that the heating rate of the particle is controlled to a large extent by the specific heat of the material.

It is to be noted from Fig. 9(b) that the slope of the temperature profiles, near the surface

$$\left(\left.\frac{\partial T}{\partial r}\right|_{r=R_0}\right)$$

are almost constant which reflects relatively little change in the external heat flux, q.

The corresponding temperature history obtained for particles of different materials and diameters suddenly immersed in plasmas of different gases and temperatures are given in Figs. 10–15.

It is noted from Fig. 10 that in a hydrogen plasma the temperature difference, ΔT_s, between the surface and the center of the particle is substantially greater than that computed for a nitrogen plasma (Fig. 9) and can reach as much as 2062 K when the surface temperature of the particle reaches its melting point. The same remarks hold for the uniform particle temperature model ('simple case') curve 3 on Fig. 10.

As expected for a particle of a good thermal conductivity material, such as copper, the heat propagation phenomena in the particle are negligible (Fig. 11). The influence of the thermal conductivity of different materials on the temperature profile across the particle is shown in Fig. 12. It can be noted that ΔT_s is negligible for W and Si and important for the oxides with low thermal conductivity such as Al_2O_3 and SiO_2.

It is interesting to note in Fig. 13 that, for an alumina particle immersed in a nitrogen plasma at 4000 K, the

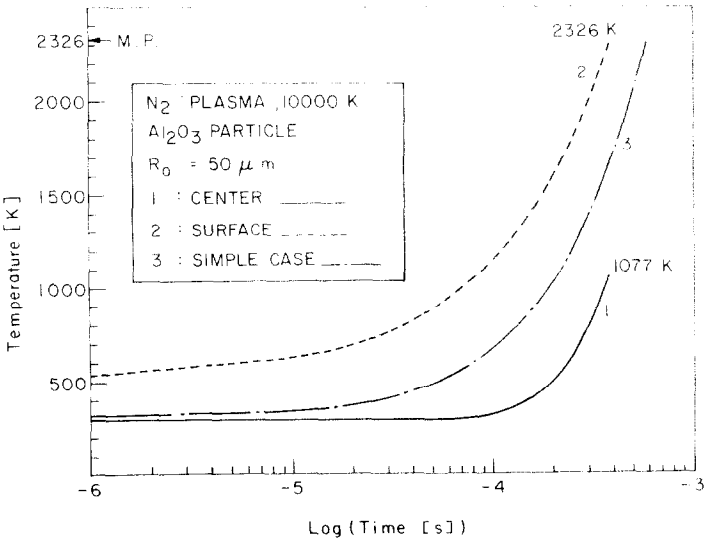

FIG. 9(a). Temperature history for a 100 μm alumina particle immersed in a nitrogen plasma at 10 000 K (including internal heat conduction).

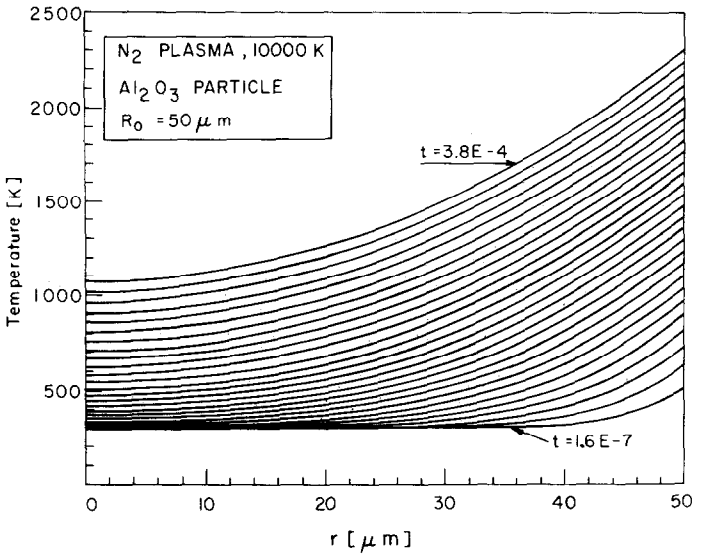

FIG. 9(b). Temperature history for a 100 μm alumina particle immersed in a nitrogen plasma at 10000 K (neglecting internal heat conduction).

temperature difference between the surface and the center of the particle is negligible compared to that obtained with a 6000 K nitrogen plasma. The effect is mainly due to the large increase in the thermal conductivity of the plasma, and thus the heat flux to the particle, over this temperature range.

The effect of the thermal conductivity of the gas is best observed by comparing ΔT_s for an alumina particle immersed respectively in a hydrogen, nitrogen and an argon plasma (Fig. 14). ΔT_s is smaller for N_2 than for H_2 and is almost negligible for Ar. ($\bar{k}$ under these conditions equals 4.6, 1.6 and 0.2 W m^{-1} K^{-1}, for N_2, H_2 and Ar, respectively.) Figure 15 shows that the diameter of the particle has relatively little influence on ΔT_s.

Due to the large differences that can develop between the temperature of the surface and that of the center of the particle, it would be most useful to have a criterion, or a parameter, that could indicate *a priori* whether this difference is negligible or not. In other words, a parameter which could indicate under which conditions internal heat propagation in the particle can be neglected and the 'simple model' can be used in calculations of the temperature history of the particle.

Based on an energy balance on the particle neglecting convective and radiative heat transfer, it can be shown that

$$\frac{\bar{k}}{R_0}(T_\infty - T_s) = k_s \left.\frac{\partial T}{\partial r}\right|_{r=R_0} \tag{26}$$

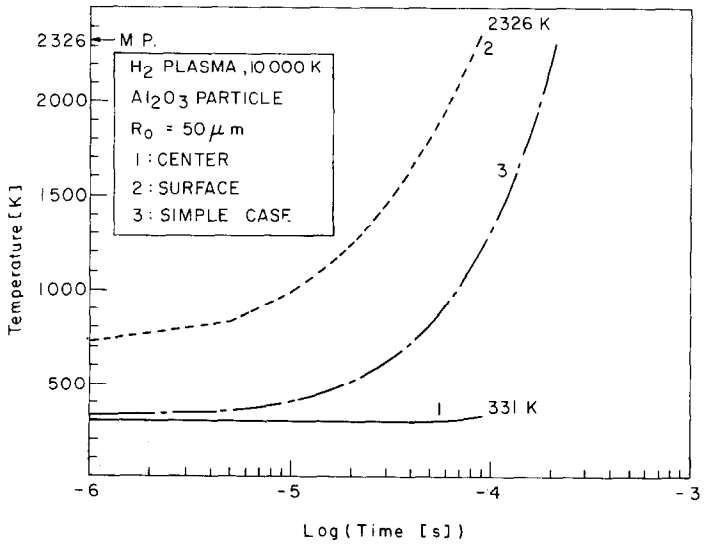

FIG. 10. Temperature history for a 100 μm alumina particle immersed in a hydrogen plasma at 10000 K (including internal heat conduction).

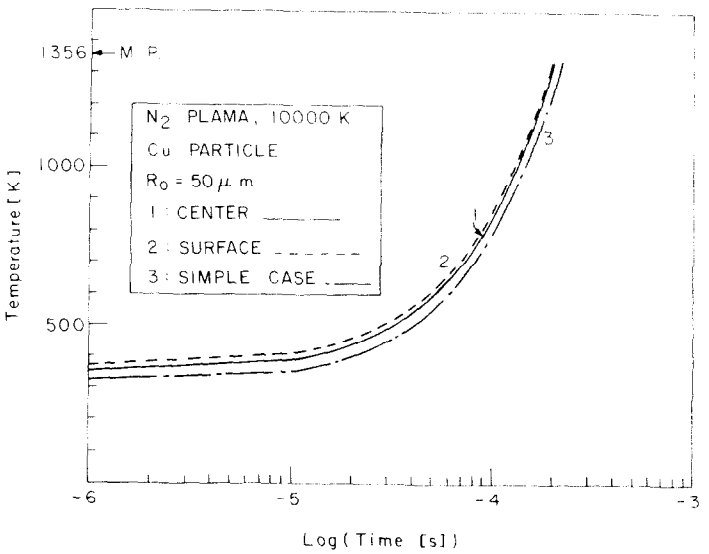

FIG. 11. Temperature history for a 100 μm copper particle immersed in a nitrogen plasma at 10000 K (including internal heat conduction).

Since

$$\left.\frac{\partial T}{\partial r}\right|_{r=R_0}$$

changes little with time during the transient heating of the particle one can write, as a first approximation, that

$$\left.\frac{\partial T}{\partial r}\right|_{r=R_0} \simeq \frac{T_s - T_c}{R_0} = \frac{\Delta T_s}{R_0}$$

or

$$\left[\frac{\Delta T_s}{T_\infty - T_s}\right] = \frac{\bar{k}}{k_s}. \tag{27}$$

It is then reasonable to expect that

$$T^* = f(Bi) \tag{28}$$

when $T^* = [\Delta T_s/(T_\infty - T_s)]$, and the Biot number,

$$Bi = \bar{k}/k_s. \tag{29}$$

In Fig. 16, T^* is plotted as a function of Bi for the different materials and plasma conditions used in our calculations. It may be noted that the temperature difference between the surface and the center of the particle is less than 5% of $(T_\infty - T_s)$ when $Bi < 0.02$.

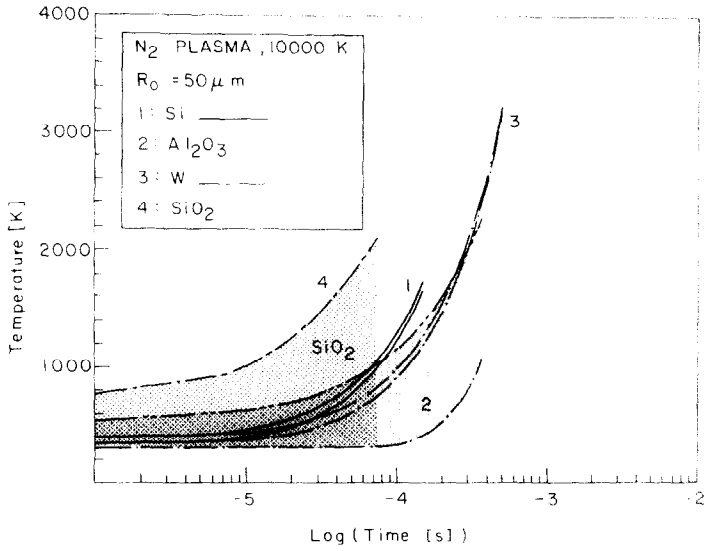

FIG. 12. Temperature histories of 100 μm diameter alumina particles of different materials immersed in a nitrogen plasma at 10000 K (including internal heat conduction).

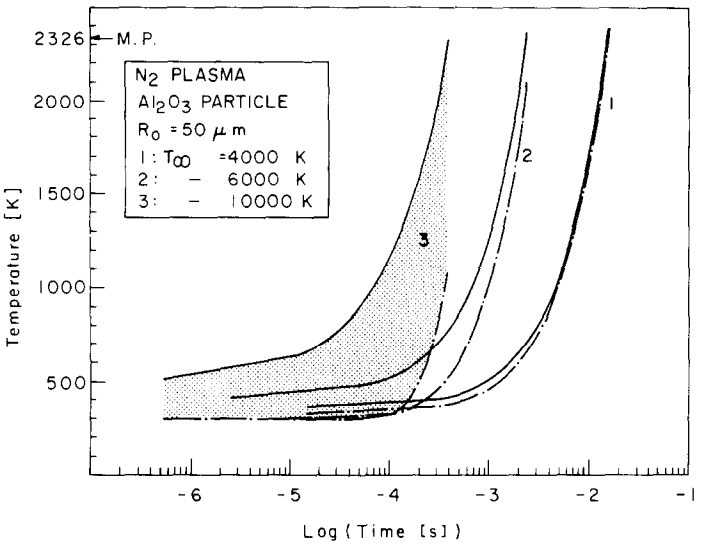

FIG. 13. Temperature histories of 100 μm diameter alumina particles immersed in a nitrogen plasma at different temperatures (including internal heat conduction).

3.3. *Heat transfer to a particle with a finite thermal conductivity in the presence of phase change*

In the previous section, dealing with the internal heat conduction in the particles, the computations were systematically stopped as the particle surface temperature reached the melting point of the material. Obviously as long as the particle remains immersed in the plasma its temperature history will proceed further with the gradual melting of the particle. In this case the melting front (limit between the solid and liquid) will propagate towards the center of the particle and the heat transfer take place across a liquid layer of increasing thickness. This could obviously result in the surface temperature of the particle increasing rapidly compared to the progression of the melting front for low thermal conductivity materials. It is then possible to reach a situation where the surface of the particle is at the boiling temperature while its center is not yet at the melting temperature.

To calculate the propagation of the melting front, one has to solve the differential problem illustrated in Fig. 17 after Murray and Landis [18]: if $r_m(t)$ is the position of the melting front at time t, one has to solve the heat transfer equations in the solid and liquid parts

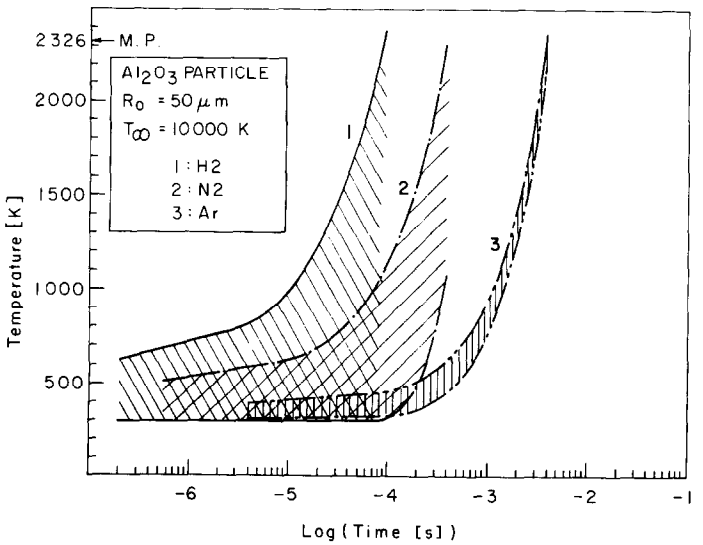

FIG. 14. Temperature histories of 100 μm diameter alumina particles immersed in different plasma gases at 10 000 K (including internal heat conduction).

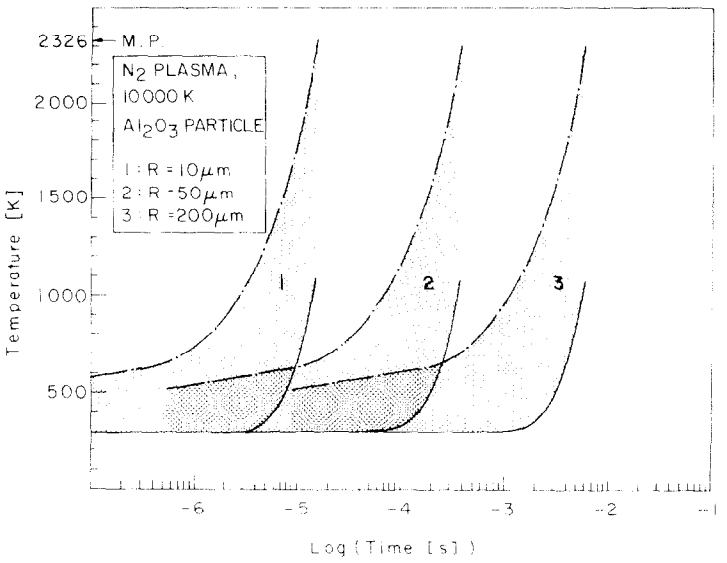

FIG. 15. Temperature histories of different diameter alumina particles immersed in a nitrogen plasma at 10000 K (including internal heat conduction).

of the particle,

$$\frac{1}{\alpha_s}\frac{\partial T}{\partial t} = \frac{1}{r^2}\left[\frac{\partial}{\partial r}\left(r^2\frac{\partial T}{\partial r}\right)\right], \tag{30}$$

$$\frac{1}{\alpha_l}\frac{\partial T}{\partial t} = \frac{1}{r^2}\left[\frac{\partial}{\partial r}\left(r^2\frac{\partial T}{\partial r}\right)\right] \tag{31}$$

with the following boundary conditions:

at $r = R_0$, $k_l\left.\frac{\partial T}{\partial r}\right|_{r=R_0} = q$, (32)

at $r = 0$, $\left.\frac{\partial T}{\partial r}\right|_{r=0} = 0$, (33)

at the solid–liquid interface,

$$\frac{dr_m}{dt} = \frac{1}{\rho\lambda_s}\left[k_l\left.\frac{\partial T_l}{\partial r}\right|_{r=r_m} - k_s\left.\frac{\partial T_s}{\partial r}\right|_{r=r_m}\right]. \tag{34}$$

The numerical technique used was that proposed by Murray and Landis [18]. It is an implicit finite-difference method with a variable grid in the radial direction (Fig. 17). The computation time was, however, improved by more than one order of magnitude using the iterative scheme proposed by Jamet [19].

The radial temperature profiles obtained during the melting of a tungsten and an alumina particle immersed in a nitrogen plasma at 10000 K are given in Figs. 18 and 19, respectively. These show two different behaviours depending on the values of the respective thermal conductivities of the particles and that of the plasma.

It is noticed that for tungsten, at the moment the particle is completely molten, its surface temperature is at 3844 K while its center is at 3680 K. On the other

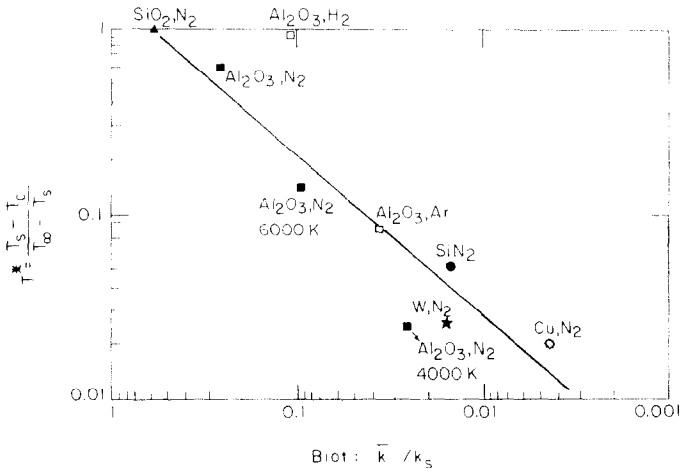

FIG. 16. T^* as function of Bi for different materials and plasma conditions. (Unless otherwise indicated, the calculations were made for 100 μm diameter particles with a plasma temperature of 10000 K.)

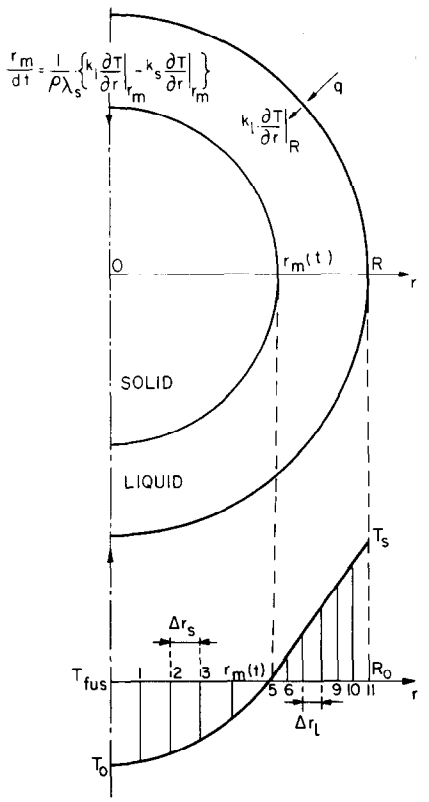

FIG. 17. Schematic showing the propagation of the melting front for a particle immersed in a plasma.

hand, the surface temperature of an alumina particle reaches its boiling point (4000 K) while the temperature of the center is still below that of the melting point of alumina (2040 K). At this point, only 92% of the particle is completely molten. The effect is even stronger when using a hydrogen plasma at 10 000 K which, because of its higher thermal conductivity, gives rise to higher heat flux to the particle surface. Under such conditions the surface of the particle has been found to reach its boiling point while the center of the particle is still at 1390 K with only 61% of the particle molten.

This could well explain the reported difficulties in obtaining a completely molten alumina plasma-sprayed coating even when measurements of the surface temperature of the particles arriving at the substrate are greater than the melting point of alumina [20].

4. EFFECT OF RADIATION HEAT LOSSES

In the preceding calculations, the radiation losses from the particle have always been neglected. In order to evaluate the maximum error introduced by such an assumption, calculations were made of the radiation energy losses, $P_{rad} = \varepsilon\sigma T_s^4$, with $\varepsilon = 1.0$, as function of the surface temperature of the particle. The results are given in Fig. 20 together with the conductive heat flux to a 100 μm diameter particle for different plasma gases and temperatures for comparison.

It may be noted that, except for a particle with a surface temperature above 2000 K immersed in an argon or nitrogen plasma below 4000 K, the radiative heat losses from the particle are negligible compared to the conductive heat flux from the plasma to the particle.

5. CONCLUSIONS

From the above theoretical analysis, the following conclusions can be made:

(1) In the presence of steep temperature gradients, the integral mean thermal conductivity of the gas must be used in the evaluation of the heat transfer coefficient,

$$\bar{k} = \frac{1}{T_\infty - T_s}\int_{T_s}^{T_\infty} k(T)\,dT. \qquad (11)$$

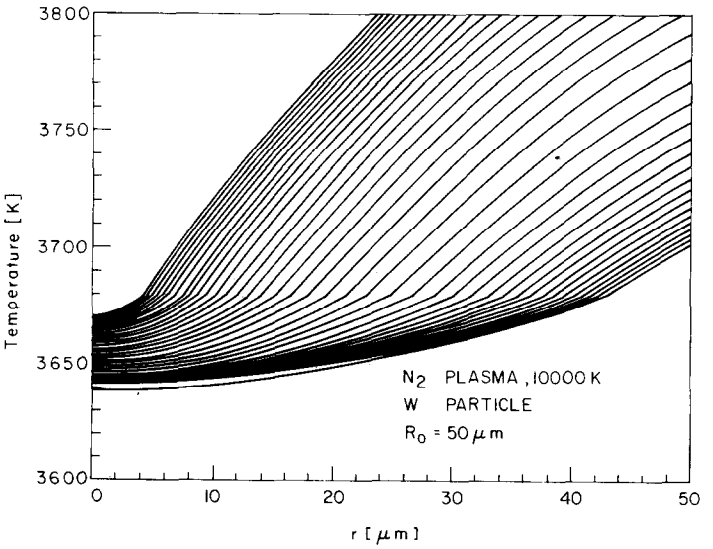

FIG. 18. Radial temperature profiles during the melting of a 100 μm diameter tungsten particle immersed in a nitrogen plasma at 10 000 K.

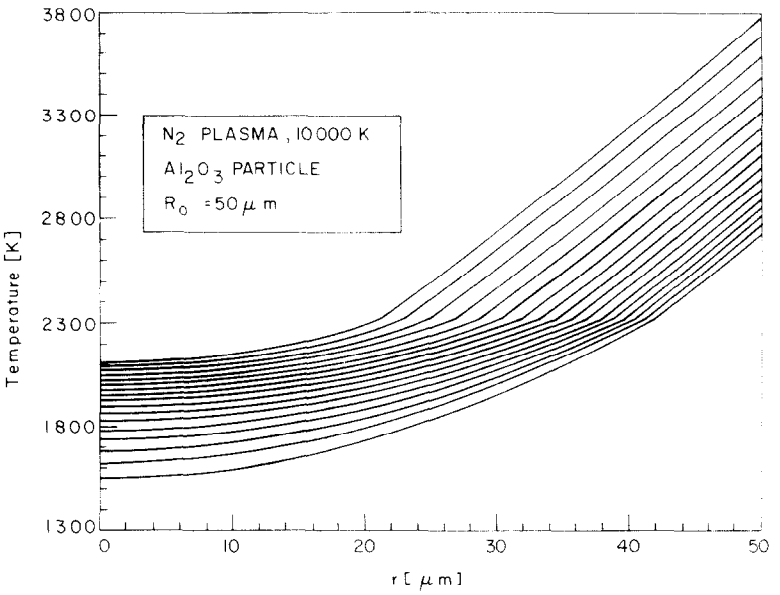

FIG. 19. Radial temperature profiles during the melting of a 100 μm diameter alumina particle immersed in a nitrogen plasma at 10000 K.

In this case, the Nusselt number for conduction heat transfer between a single sphere and an infinite stream is equal to 2.0.

(2) For a sphere suddenly immersed in a thermal plasma, the relaxation time of the thermal boundary layer around the sphere is orders of magnitude smaller than its transient heating time. The use of a Nusselt number of 2.0 for the calculation of the conductive heat transfer rate to the particle is therefore quite adequate.

(3) During the transient heating of a particle under

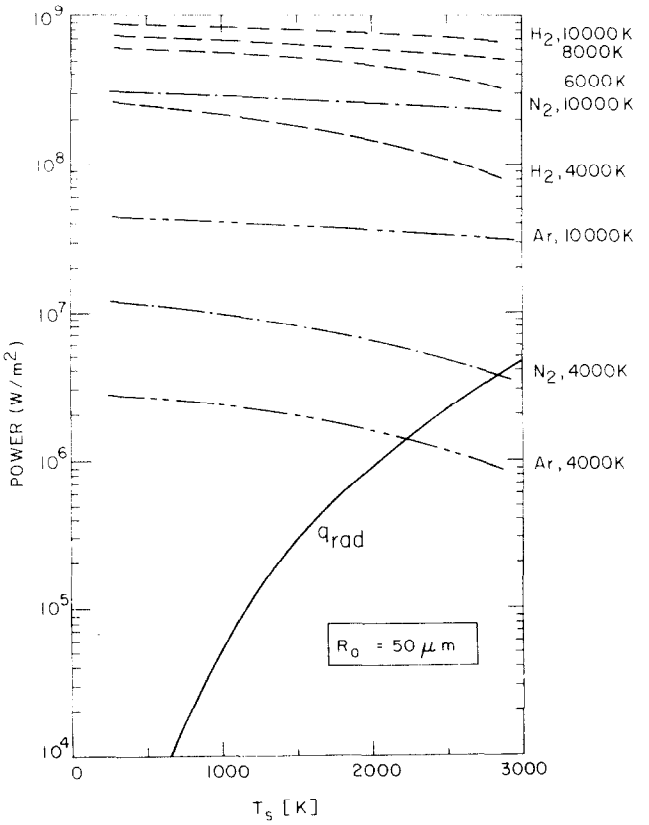

FIG. 20. Radiative heat flux from the particle to the surrounding as function of the particle surface temperature.

plasma conditions, internal heat conduction in the particle should be taken into account if the Biot number is greater than 0.02. Depending on the thermal conductivity of the plasma gas and that of the particle, temperature differences as high as 1000 K can develop between the surface and the center of the particle even for a particle as small as 20 μm in diameter.

(4) For poor heat conducting materials such as alumina, the surface temperature of a 100 μm diameter particle immersed in a hydrogen plasma at 10000 K, can reach the boiling point of alumina ($T = 4000$ K) while its center is still in the solid state ($T_c < 2040$ K).

(5) Except for a particle with a surface temperature above 2000 K immersed in an argon or nitrogen plasma of a temperature below 4000 K, radiation heat losses from the particle to the surrounding are negligible compared to the conductive heat flux from the plasma to the particle.

REFERENCES

1. N. N. Rykalin and V. V. Kudinov, Plasma spraying, *Pure Appl. Chem.* **48,** 229–239 (1976).
2. J. L. Besson and P. Boch, Plasma spraying of ceramics, International Round Table Discussion on Special ceramics for Electronic and Electrical Engineering, Warsaw, 8–11 October (1978).
3. A. Vardelle, P. Fauchais et M. Vardelle, Projection de revêtements protecteurs par plasma. *Actual. Chim.* **10,** 69 (1981).
4. M. G. Fey, C. B. Wolf and F. J. Harvey, Magnetic spheroidization using an A. C. arc heater, International Round Table, Transport Phenomena in Thermal Plasmas, Odeillo, France, 12–16 September (1975).
5. N. N. Sayegh and W. H. Gauvin, Numerical analysis of variable property heat transfer to a single sphere in high temperature surrounding, *A.I.Ch.E. Jl* **25,** 522–534 (1979).
6. C. Borgianni, M. Capitelli, F. Cramarossa, L. Triolo and E. Molinari, The behaviour of metal oxides injected into an argon induction plasma, *Combustion and Flame* **13,** 181–194 (1976).
7. C. Bonet, M. Daguenet et P. Dumargue, Etude théorique de l'évaporation d'une particule sphérique d'un matériau réfractaire dans un plasma thermique, *Int. J. Heat Mass Transfer* **17,** 643–654 (1974).
8. C. Bonet, Thermal plasma processing, *CEP* **72,** 63–69 (1976).
9. M. I. Boulos and W. H. Gauvin, Powder processing in a plasma jet, a proposed model, *Can. J. Chem. Engng* **52,** 355–363 (1979).
10. M. I. Boulos, Heating of powders in the fire-ball of an inductive plasma, *IEEE Trans. Plasma Sci.* **4,** 93–106 (1978).
11. D. Bhattacharyya and W. H. Gauvin, Modelling of heterogenous systems in a plasma jet reactor, *A.I.Ch.E. Jl* **21,** 879–885 (1975).
12. T. Yoshida and K. Akaski, Particle heating in a radio-frequency plasma torch, *J. Appl. Phys.* **48,** 2252–2260 (1977).
13. J. K. Fiszdon, Melting of powder grains in a plasma flame, *Int. J. Heat Mass Transfer* **22,** 749–761 (1979).
14. M. Vardelle, A. Vardelle, P. Fauchais and M. I. Boulos, Plasma-particle momentum and heat transfer: modelling and measurements, *A.I.Ch.E. Jl*, in press (1982).
15. E. Bourdin, A. Vardelle, M. Vardelle, M. I. Boulos and P. Fauchais, Computer modelisation of heat and momentum transfer between a particle and a D.C. plasma jet, *Proc. 5th Int. Symp. Plasma Chemistry*, Edinburgh, 10–14 August, pp. 804–815 (1981).
16. Y. C. Lee, K. C. Hsu and E. Pfender, Modelling of particles injected into a d.c. plasma jet, *Proc. 5th Int. Symp. Plasma Chemistry*, Edinburgh, 10–14 August, pp. 795–803 (1981).
17. P. H. Vaessen, J. Arts and J. M. Houben, Energy and momentum transfer to micron sized particles in an atmospheric argon plasma jet for plasma spraying, *Proc. 5th Int. Symp. Plasma Chemistry*, Edinburgh, 10–14 August, pp. 115–119 (1981).
18. W. D. Murray and F. Landis, Numerical and machine solutions of transient heat-conduction problems involving melting or freezing—Part I. Method of analysis and sample solutions, *Trans. Am. Soc. Mech. Engrs.* Series C, *J. Heat Transfer* **81,** 106–112 (1959).
19. R. Bonnerot and P. Jamet, A second order finite element method for the one-dimensional Stefan problem, *Int. J. Numer. Methods Engng* **8,** 811–820 (1974).
20. M. Vardelle, A. Vardelle, J. L. Besson and P. Fauchais, Correlations entre les propriétés des dépôts et les conditions de fonctionnement d'une installation de projection; un exemple, l'alumine, *Rev. Phys. Appl.* **16,** 425–434 (1981).

CONDUCTION DE LA CHALEUR EN REGIME TRANSITOIRE DANS UN MILIEU PLASMA

Résumé—Nous avons développé une analyse théorique des différents phénomenes intervenant et des hypothèses généralement utilisées pour le calcul du transfert de chaleur entre un plasma thermique et une sphère de matière condensée isolée. En présence des gradients de température très importants recontrés dans de tels milieux, nous avons montré, que si nous utilisions la valeur intégrée moyenne de la conductivité thermique du plasma pour évaluer le coefficient de transfert de chaleur, le nombre de Nusselt pour le transfert de chaleur conductif entre le plasma et la particule est rigoureusement égal à 2. Nos résultats montrent également que le temps de relaxation de la couche limite thermique entourant la particule est négligeable par rapport au temps de chauffage de la particule.

Des calculs ont été menés pour des particules de différents diamètres (20 à 100 μm) et des matériaux différents (Al_2O_3, W, Si, Cu ...) immergés dans des plasmas d'argon, d'azote et d'hydrogene dont les températures varient de 4000 à 10000 K ces calculs montrent que pour des nombres de Biot supérieurs à 0,02, des différences de température aussi élevées que 1000 K peuvent exister entre la surface et le centre de la particule, même pour des particules de diamètre inférieur à 20 μm. Dans quelques cas, lorsque le flux de chaleur est particulièrement élevé, (plasma d'hydrogène à 10000 K), la température de surface d'une particule d'alumine de 100 μm de diamètre peut atteindre la température de vaporisation de l'alumine (4000 K) alors que son centre est encore à l'état solide.

Les résultats d'une analyse relativement simple montrent que, excepté pour une particule dont la température de surface est supérieure à 2000 K immergée dans un plasma d'argon ou d'azote en dessous de 4000 K, les pertes par rayonnement de la particule sont négligeables comparées au flux de chaleur conductif apporté par le plasma à la particule.

INSTATIONÄRE WÄRMELEITUNG UNTER PLASMA-BEDINGUNGEN

Zusammenfassung – Die verschiedenen Phänomene, die beim Wärmeübergang an einer Einzelkugel unter Plasma-Bedingungen auftreten, wurden theoretisch untersucht, ebenso die Annahmen, die bei der Berechnung gemacht werden. Es wird gezeigt, daß bei der Berechnung des Wärmeübergangskoeffizienten mit der integralen mittleren Wärmeleitfähigkeit des Plasmas beim Auftreten steiler Temperatur-Gradienten die Nusselt-Zahl für den Wärmeübergang durch Wärmeleitung zwischen Plasma und Partikel gleich 2.0 ist. Die Ergebnisse zeigen außerdem, daß die Relaxationszeit der thermischen Grenzschicht an den Partikeln vernachlässigbar klein ist, verglichen mit der Dauer ihrer instationären Aufheizung. Die Berechnungen wurden für Partikel von unterschiedlichem Durchmesser (20 bis 100 μm) und aus unterschiedlichem Material (Al_2O_3, W, Si, Cu...) durchgeführt, die von Argon-, Stickstoff- und Wasserstoff- Plasma bei Temperaturen zwischen 4000 und 10000 K umgeben waren. Sie zeigen, daß sich für Biot-Zahlen größer als 0,02 zwischen Oberfläche und Kern der Partikel Temperaturdifferenzen bis zu 1000 K entwickeln können, sogar für Partikel mit Durchmessern von nur 20 μm. In wenigen Fällen, wenn die Wärmestromdichte besonders hoch ist (Wasserstoff-Plasma bei 10000 K), kann die Oberfläche eines 100 μm-Aluminium-Partikels die Siedetemparatur des Aluminiums (4000 K) erreichen, während sich der Kern noch in festem Zustand befindet.

Die Ergebnisse einer verhältnismäßig einfachen Analyse zeigen, daß – außer bei Partikeln mit einer Oberflächentemperatur über 2000 K, die sich in Argon- oder Stickstoff-Plasma von unter 4000 K befinden – die Wärmeverluste durch Strahlung vom Partikel in seine Umgebung vernachlässigbar sind, verglichen mit dem Wärmestrom durch Wärmeleitung vom Plasma an die Partikeloberfläche.

НЕСТАЦИОНАРНАЯ ТЕПЛОПРОВОДНОСТЬ В УСЛОВИЯХ ОБРАЗОВАНИЯ ПЛАЗМЫ

Аннотация — Проведен теоретический анализ различных экспериментальных результатов и допущений, используемых при расчете интенсивности переноса тепла к единичной сфере в условиях образования плазмы. В случае больших градиентов температур показано, что если при расчете коэффициента теплопереноса используется среднеинтегральный коэффициент теплопроводности плазмы, значение числа Нуссельта для процесса передачи тепла теплопроводиостью между плазмой и частицей равно 2,0. Из результатов также следует, что время релаксации теплового пограничного слоя вокруг частицы пренебрежимо мало по сравнению с соответствующим временем нестационарного нагрева. Расчеты выполнены для частиц различных диаметров (от 20 до 100 мкм) и материалов (Al_2O_3, W, Si, Cu...), помещенных в плазму аргона, азота и водорода в диапазоне температур от 4000 до 10000 К. Показано, что при значениях числа Био, превышающих 0,02, разность температур между поверхностью и центром частицы может достигать 1000 К даже для сфер самого малого диаметра (20 мкм). В ряде случаев, когда тепловой поток особенно велик (плазма водорода при 10000 К), температура поверхности алюминиевой частицы диаметром 100 мкм может достигать точки плавления алюминия (4000 К), а центр ее все еще оставаться в твердом состоянии.

Результаты довольно простого анализа показывают, что за исключением частицы с температурой поверхности выше 2000 К, помещенной в плазму аргона или азота с температурой ниже 4000 К, лучистые потери тепла от частицы в окружающую среду пренебрежимо малы по сравнению с передачей тепла теплонроводностью от плазмы к частице.